arXiv:0808.3846v1 [astro-ph] 28 Aug 2008

Suzaku Observations of SGR 1900+14 and SGR 1806−20

Yujin E. Nakagawa[1,2] Tatehiro Mihara[1] Atsumasa Yoshida[2] Kazutaka Yamaoka[2]
Satoshi Sugita[2] Toshio Murakami[3] Daisuke Yonetoku[3] Motoko Suzuki[4]
Motoki Nakajima[5] Makoto Tashiro[6] and Kazuhiro Nakazawa[7]

[1]*Institute of Physical and Chemical Research (RIKEN), 2-1 Hirosawa, Wako, Saitama 351-0198*
yujin@crab.riken.jp
[2]*Graduate School of Science and Engineering, Aoyama Gakuin University, 5-10-1 Fuchinobe,*
Sagamihara, Kanagawa 229-8558
[3]*Department of Physics, Kanazawa University, Kakuma, Kanazawa, Ishikawa 920-1192*
[4]*Tsukuba Space Center, 2-1-1 Sengen, Tsukuba, Ibaraki 305-8505*
[5]*College of Science and Technology, Nihon University, 1-8-14 Kanda-Surugadai,*
Chiyoda-ku, Tokyo 101-0062
[6]*Department of Physics, Saitama University, 255 Shimo-Okubo, Sakura-ku, Saitama,*
Saitama 338-8570
[7]*Department of Physics, University of Tokyo, 7-3-1 Hongo, Bunkyo-ku, Tokyo 113-0033*

Abstract

Spectral and timing studies of *Suzaku* ToO observations of two SGRs, 1900+14 and 1806−20, are presented. The X-ray quiescent emission spectra were well fitted by a two blackbody function or a blackbody plus a power law model. The non-thermal hard component discovered by INTEGRAL was detected by the PIN diodes and its spectrum was reproduced by the power law model reported by INTEGRAL. The XIS detected periodicity $P = 5.1998 \pm 0.0002$ s for SGR 1900+14 and $P = 7.6022 \pm 0.0007$ s for SGR 1806−20. The pulsed fraction was related to the burst activity for SGR 1900+14.

Key words: stars: pulsars individual(SGR 1900+14, SGR 1806−20)

1. Introduction

Magnetars (neutron stars with a super strong surface magnetic field $B \sim 10^{15}$ G – e.g., Duncan & Thompson 1992; Paczyński 1992) have received considerable attention recently. The magnetar's field strength exceeds the critical field $B_c \equiv m_e^2 c^3 / c\hbar \approx 4.4 \times 10^{13}$ G, and hence the non-linear effects of quantum electrodynamics must be considered in the processes of radiation transfer. Several studies have now found X-ray sources which are magnetar candidates, namely the soft gamma repeaters (SGRs) and anomalous X-ray pulsars (AXPs). They display X-ray quiescent emission with luminosities $L = 10^{33}$-10^{35} erg s^{-1} (e.g., Woods & Thompson 2006). The SGRs and a few AXPs also exhibit "short bursts" with typical durations $\Delta t \sim 100$ ms and super-Eddington luminosities $L \sim 10^{40}$ erg s^{-1}. One of the most remarkable burst phenomena is giant flares from SGRs. Three SGRs have emitted giant flares over the past three decades. The most energetic one had $L \sim 5 \times 10^{47}$ erg s^{-1}, from SGR 1806−20 on 27 December 2004 (Terasawa et al. 2005). The giant flares have been proposed as candidates for some short gamma-ray bursts (GRB) with durations $\Delta t \lesssim 2$ s (e.g., Hurley et al. 2005). Delayed X-ray and radio emission following giant flares or short bursts display similar behavior to GRB afterglows (Frail et al. 1999; Feroci et al. 2003; Cameron et al. 2005; Nakagawa et al. 2008), which may also support this hypothesis.

Two spectral models, a two blackbody function (2BB) and a blackbody plus a power law model (BB+PL), have been suggested for the quiescent X-ray emission of the magnetar candidates. A comprehensive study of many short SGR bursts detected by the High Energy Transient Explorer 2 (HETE-2) has shown that 2BB is preferable, although it is an empirical model (Nakagawa et al. 2007a). Although a physical model for the energy spectra remains controversial despite observations by several satellites, strong linear correlations between the lower and higher blackbody temperatures (kT_{LT}, kT_{HT}), and between the lower and higher blackbody radii (R_{LT}^2, R_{HT}^2) were found, irrespective of the activity states (i.e., the X-ray quiescent emission or the short bursts), using 2BB (Nakagawa et al. 2007b). There are various theoretical models which reproduce the spectra of the quiescent X-ray emission (e.g., Perna et al. 2001; Güver, Özel & Lyutikov 2006). Even more exotic models have been proposed, such as that invoking a p-star (Cea 2006).

One piece of evidence in favor of the magnetar model is that magnetic pressure confines the photon-pair plasma from the giant flare in a (rather) small volume close to the neutron star (Thompson & Duncan 1995). One complication is the fact that there has not been a secure direct measurement of the magnetic field of a magnetar candidate. One possible such measurement is an absorption feature interpreted to be due to proton cyclotron resonance scattering which has been seen in a spectrum of the

precursor emission of a ~ 1.5 s burst from SGR 1806−20 (Ibrahim et al. 2002). This kind of feature can also be seen in the spectrum of X-ray quiescent emission from AXP 1RXS J170849−400910 (Rea et al. 2003). The lack of this feature in most magnetar candidates may be explained by a model which smears the absorption feature due to multiple cyclotron resonant scatterings in a stellar atmosphere and its magnetosphere (Güver, Özel & Lyutikov 2006).

Several studies have reported periods $P = 5$-13 s and period derivatives $\dot{P} = 10^{-11}$-10^{-13} s s^{-1} for the magnetar candidates (Woods & Thompson 2006). It is known that pulse characteristics such as the pulsed fraction and pulse shape vary in time (e.g., Woods et al. 2007), and involve complex pulse morphology. However, little has been done to elucidate the underlying physics of the pulse characteristics. A recent theoretical study suggests that the pulse characteristics may be explained by trapped fireballs produced by starquakes (Jia et al. 2008).

This paper reports the broadband spectroscopy of two SGRs, 1900+14 and 1806−20, observed by *Suzaku*. The relation between pulsed fraction and burst rate will also be discussed. The distances are assumed to be 14.5 kpc for SGR 1900+14 (Hurley et al. 1999; Vrba et al. 2000) and 8.7 kpc for SGR 1806−20 (Corbel et al. 1997; Corbel & Eikenberry 2004; Cameron et al. 2005; McClure-Griffiths & Gaensler 2005; Bibby et al. 2008).

2. Observations

Suzaku (Mitsuda et al. 2007) has the capability of giving high quality broadband spectra of astrophysical X-ray and gamma-ray sources, because of the great sensitivity of the X-ray imaging spectrometer (XIS; 0.2-12 keV; Koyama et al. 2007) and an extremely low background level of the hard X-ray detector (HXD; 10-700 keV; Takahashi et al. 2007). The XIS consists of one back-illuminated (BI) CCD and three front-illuminated (FI) CCDs. The HXD consists of PIN diodes (10-70 keV) and GSO units (40-600 keV). The XIS has an effective area of 370 cm^2 (BI) and 330 cm^2 (FI) at 8 keV. Although the effective areas are comparable to the EPIC on-board XMM-*Newton*, XIS has better energy resolution below 1 keV: $\sim$50 eV (BI) and $\sim$40 eV (FI) at 0.525 keV. The HXD PIN also has better energy resolution, $\sim$3 keV, compared with FREGATE[1] on-board HETE-2 (5 keV at 20 keV) and IBIS on-board INTEGRAL (7 keV at 100 keV; Winkler 1999). *Suzaku* can observe objects in the energy range 0.2-600 keV which covers a lower X-ray band compared with HETE-2 (2-400 keV; Ricker et al. 2003) and INTEGRAL IBIS (15 keV-10 MeV; Winkler 1999). Since the HXD field of view is narrow (34′ × 34′), it has good sensitivity to weak sources. The sensitivity of the HXD is 3×10^{-6} photons s^{-1} keV^{-1} cm^{-2} at 20 keV (Takahashi et al. 2007), which is better than HETE-2 FREGATE ($\sim 10^{-3}$ photons s^{-1} keV^{-1} cm^{-2} at

100 keV; Atteia et al. 2003) and INTEGRAL IBIS[2] (10^{-5} photons s^{-1} keV^{-1} cm^{-2} at 20 keV).

When the SGRs 1900+14 and 1806−20 displayed intense bursting activity, scheduled target of opportunity (ToO) observations by *Suzaku* were performed. Table 1 shows a summary of the observations.

SGR 1900+14 began a very high burst activity on 29 March 2006, and *Swift* recorded more than 40 bursts on that day (Israel et al. 2008). The *Suzaku* ToO observation started at 8:43 and ended at 21:52 on 1 April 2006 (UT). The X-ray quiescent emission was detected by the XIS, but there was no significant emission in the HXD data. No burst was found in the XIS and HXD light curves. There were no *Swift* bursts during the *Suzaku* observation (the bottom right panel in figure 3).

A bright long burst from SGR 1806−20 was detected by Konus-Wind and *Suzaku*-WAM on 26 March 2007 (Golenetskii et al. 2007). The *Suzaku* ToO observation of this source started at 15:08 on 30 March 2007 and ended at 1:30 31 March 2007 (UT). Both the X-ray quiescent emission and the non-thermal hard X-ray emission discovered by INTEGRAL (Molkov et al. 2005) were detected by the XIS and the HXD. Two dim short bursts were detected by *Suzaku*. One of them was a short burst localized by *Swift* at 16:14:38, and the other was detected only by *Suzaku* at 17:34:00. Since these bursts are too weak to perform spectral analyses, we do not consider them further here.

3. Analysis

3.1. Data Reduction

The reduction of both the XIS and HXD event data (v2.0) were made using HEAsoft 6.4.1 software. The latest calibration database (CALDB: 20080616) was applied to the unfiltered XIS event data using *xispi* (v2008-04-10). Then the new data were filtered using the basic criteria[3] and with a grade selection "GRADE = (0,2-4,6)" using *xselect* (v2.4a). After that, hot and flickering pixels were removed using *cleansis* (v1.7). Telemetry saturated time intervals were estimated by *xisgtigen* (v2007-05-14), and the time intervals were removed using *xselect*. The sizes of the source and background regions are summarized in table 1. The background regions of the FI CCDs for the SGR 1806−20 observation are selected near the edge opposite to the source region (because the object fell on the edge), while those of the other CCDs were selected near both edges. Light curves and spectra were extracted from the clean XIS event data using *xselect*. The response matrix files were created by *xisrmfgen* (v2007-05-14) and the ancillary response function files were generated by *xissimarfgen* (v2008-04-05). The spectra were binned to at least 50 counts in each spectral bin by *grppha*.

The barycentric correction was applied to the cleaned XIS event data by use of *aebarycen*. Then 0.2-12 keV light curves with 1 s binning (the minimum time resolution of the XIS 1/8 window mode) were extracted using

---

[1] See http://space.mit.edu/HETE/fregate.html.

[2] See http://integral.esa.int/integ_payload_imager.html.
[3] The XIS basic criteria were derived from http://suzaku.gsfc.nasa.gov/docs/suzaku/analysis/abc.

the source and background regions for the spectra. To find the most reliable period, timing analyses were performed by *powspec* and *efsearch*. A folded light curve was made with the best period by *efold*.

The latest calibration database (CALDB: 20080602) was applied to the unfiltered HXD event data using *hxdpi* and *hxdgrade*. The PIN and GSO event data were extracted from the newly calibrated data with basic criteria[4] using *xselect*. The tuned background event data (bgd_d) were utilized to estimate the non X-ray background (NXB). The cosmic X-ray background (CXB) was estimated based on the HEAO-1 result (Boldt 1987). Then the good time interval (GTI) files were generated by merging the PIN/GSO GTI extension and the bgd_d GTI extension using *mgtime*. Light curves and spectra were extracted using *xselect*. For the source spectra, the dead time corrections were applied using *hxddtcor*. The modeled background event data (bgd_d) were utilized in our analyses. The spectra were binned to at least 30 counts in each spectral bin by *grppha*.

Since both SGRs 1900+14 and 1806−20 are located in the galactic plane, the galactic ridge emission (GRE) should be considered as well as NXB and CXB. It is not easy to estimate the contribution of the GRE, so we used the HESS J1804−216 BGD data (Bamba et al. 2007) to estimate both the CXB and GRE for the SGR 1806−20 observation. Note that all PIN diodes were operated at 500 V during the HESS J1804−216 BGD observation, while half of the PIN diodes (UNITID$\lesssim$7) were operated at 400 V during the SGR 1806−20 observation. Since simultaneous analysis of these two observations with different modes is not available, we concentrate on the 500 V data (i.e., UNITID>7).

3.2. Spectral Analysis

Since a two blackbody function (2BB) and a blackbody plus a power law model (BB+PL) have been suggested for the quiescent SGR X-ray spectra, we used them for our spectral analyses. An absorption model was applied to both models.

The XIS spectra of SGR 1900+14 are acceptably fitted by 2BB and BB+PL, for which the spectral parameters are summarized in table 3, and the spectra are shown in figure 1 (a).

The non-thermal hard X-ray emission component discovered by INTEGRAL (Molkov et al. 2005) was detected by the PIN diodes for SGR 1806−20. The emission is significant even if we increase the background flux by a factor of 1.02 (corresponding to the current background fluctuation of the PIN diodes). Since there are not enough statistics to investigate the spectral shape of the non-thermal hard emission, we performed a spectral analysis using a power law model (HPL) with a fixed index of $\Gamma = 1.6$ as measured by INTEGRAL. The 10-70 keV flux was $F = 2.9^{+0.9}_{-1.2} \times 10^{-11}\,\mathrm{erg\,cm^{-2}\,s^{-1}}$, where the quoted errors are 68% confidence levels. The unabsorbed 1-200 keV

flux was estimated to be $F \sim 4.3 \times 10^{-11}\,\mathrm{erg\,cm^{-2}\,s^{-1}}$ using the best-fit spectral parameters which is lower by a factor of ~ 3 than the flux observed by INTEGRAL ($F \sim 1.3 \times 10^{-10}\,\mathrm{erg\,cm^{-2}\,s^{-1}}$; Molkov et al. 2005). Then we performed the broadband spectral analyses of the XIS and the PIN diodes for SGR 1806−20. The spectra are well described by 2BB plus HPL (2BB+HPL) or BB+PL plus HPL (BB+PL+HPL). The index and flux of the non-thermal hard emission are fixed to $\Gamma = 1.6$ and $F = 2.9 \times 10^{-11}\,\mathrm{erg\,cm^{-2}\,s^{-1}}$, respectively. The broadband spectra of SGR 1806−20 are shown in figure 1 (b).

3.3. Timing Analysis

The pulse period of SGR 1900+14 was searched for using the XIS 0.2-12 keV light curves. Two candidates with nearly the same confidence level were found from an epoch-folding analysis: $P = 5.1998 \pm 0.0002\,\mathrm{s}$ ($\chi^2 = 24.8$) and $P = 5.2043 \pm 0.0003\,\mathrm{s}$ ($\chi^2 = 24.7$). The folded light curve with the first period shows a pulsation (the left panel in figure 2), while the other case does not display a clear pulsation (not shown in figure 2). In addition, the first pulse period is consistent with that determined by XMM-*Newton* on April 1 2006 (Mereghetti et al. 2006), the same date as that of the *Suzaku* observation. The most plausible pulse period is therefore $P = 5.1998 \pm 0.0002\,\mathrm{s}$. The pulse period derivative between the XMM-*Newton* observation in September 2005 ($P = 5.198346 \pm 0.000003\,\mathrm{s}$; Mereghetti et al. 2006) and the *Suzaku* observation in April 2006 is estimated to be $\dot{P} = (8.7 \pm 1.2) \times 10^{-11}\,\mathrm{s\,s^{-1}}$. This is lower by a factor of 0.8 than the first measurement ~ 100 days prior to the giant flare on 27 August 1998 (Kouveliotou et al. 1999). Using the folded light curve with the best period, the pulsed fraction is found to be $P_\mathrm{f} = 16 \pm 3\%$. Here $P_\mathrm{f} = (C_\mathrm{max} - C_\mathrm{min})/(C_\mathrm{max} + C_\mathrm{min})$, where C_max and C_min are the measured count rates at the maximum and at the minimum, respectively.

The pulse period of SGR 1806−20 from an epoch-folding analysis is found to be $P = 7.6022 \pm 0.0007\,\mathrm{s}$ ($\chi^2 = 53.1$) using XIS 0.2-12 keV light curves. The folded light curve displays the pulsations, as shown in the left panel in figure 2. Comparing this with the reported pulse period derived from the XMM-*Newton* observation on September 10 2006 ($P = 7.5891 \pm 0.0002\,\mathrm{s}$; Esposito et al. 2007), the pulse period derivative is estimated to be $\dot{P} = (7.5 \pm 0.4) \times 10^{-10}\,\mathrm{s\,s^{-1}}$. This is consistent with previously reported values derived from observations after the giant flare on 27 December 2004 (e.g., Woods et al. 2007). Using the folded light curve, the pulsed fraction is found to be $P_\mathrm{f} = 8 \pm 2\%$.

4. Discussion and Conclusion

The quiescent emission spectra of the SGRs 1900+14 and 1806−20 measured by the XIS on-board *Suzaku* are well described by either a two blackbody function (2BB) or a blackbody plus a power law model (BB+PL). The 2BB temperatures (kT_LT and kT_HT) and radii (R^2_LT and R^2_HT) show good agreement with the kT_LT-kT_HT and R^2_LT-R^2_HT correlations reported by Nakagawa et al. (2007b).

---

4   The   HXD   basic   criteria   were   taken   from
      http://www.astro.isas.ac.jp/suzaku/analysis/7step_HXD_20080501.html

A shallow dip is apparent at around 2.3 keV in the SGR 1900+14 spectra as shown in figure 1 (a). However, the XIS hardware team has cautioned that the detector gain has some unresolved uncertainties around 2 keV for the window mode[5], so this dip might not be real. If we treat it as a line feature, however, it could be well represented by a Gaussian shape absorption with $E = 2.3 \pm 0.1$ keV and $\sigma = 0.2^{+0.2}_{-0.1}$ keV, where E is the line energy and σ is the line width. If the dip is due to the fundamental absorption feature of proton cyclotron resonant scatterings, the dipole magnetic field is $B = 3.7 \times 10^{14}(E/2.3 \, \text{keV})$ G. We conducted an absorption line search for both SGRs 1900+14 and 1806−20 using a narrow Gaussian absorption line model with the line center as a free parameter ranging from 0.2 keV to 12 keV. No feature was found except for the above mentioned $E \sim 2.3$ keV shallow dip of SGR 1900+14. The upper limits of the feature are $\tau < 0.3$ (SGR 1900+14) and $\tau < 0.4$ (SGR 1806−20).

The non-thermal hard X-ray emission of SGR 1806−20, discovered by INTEGRAL in a 1.6 Ms long observation, was detected by the PIN diodes on-board $Suzaku$ with a short exposure time (~ 20 ks) because of the good sensitivity and the very low background level of this instrument.

The periodicities of SGRs 1900+14 and 1806−20 (table 2) are detected despite the short exposure time (~ 20 ks), again because of the low background level of the $Suzaku$ XIS. It has been recognized that the pulsed fractions of SGRs are not stable, and that their pulse shapes are complicated. One example is the fact that the pulsed fraction displayed a clear drop-off around the day of the giant flare from SGR 1806−20 on 27 December 2004 (Woods et al. 2007). To perform a deeper study of the pulse characteristics of SGR 1900+14, we compared the pulsed fractions to the X-ray fluxes and burst rate. The pulsed fractions and the X-ray fluxes have been derived both from our work (tables 2 and 3) and from the literature (Mereghetti et al. 2006; Esposito et al. 2007; Israel et al. 2008), while the burst rate was estimated from the list on the IPN web site[6]. Panel (a) in figure 3 shows their time histories over 10 years from 1997 to 2007, where A, B and C indicate the days of the giant flare on 27 August 1998, the intermediate flare on 18 April 2001 and the extraordinary burst activity with more than 40 bursts on 29 March 2006, respectively. The results of the $Suzaku$ observation are plotted with star symbols.

There seems to be drop-off of the pulsed fraction around the days of B and C. Panels (b) and (c) in figure 3 give an expanded view of panel (a) for days B and C, respectively. In panels (b) and (c), the pulsed fractions display a clear drop-off after both active days (i.e., B and C). No burst activity was found after the day B for 9 days, and then the quiet burst activity appeared. Since the day C, the burst activity had been gradually disappearing. No bursts were reported by the IPN during the $Suzaku$ observation (the star symbol in figure 3). The known

bursts before and after the $Suzaku$ observation were detected at 12:19:51 on 29 March 2006 and at 00:23:48 on 5 April 2006, respectively. On the contrary, SGR 1806−20 displayed one burst during the $Suzaku$ observation, and moderate, steady burst activity before and after it. This drop-off is found in response not only to the giant flare but also to the extraordinary burst activity. (This implies that the pulsed fraction is related to burst activity.) One possible explanation is to assume that magnetic confinement stores a vast amount of energy in the neutron star atmosphere or magnetosphere through energy injections such as starquakes, and that the pulsed fraction is then increased. After that the stored energy may be released as bursts either through reconnection, or some sort of instability such as the thermonuclear explosions of X-ray bursts. A recent theoretical study reports that a variety of pulse morphologies can be caused by trapped fireballs released by starquakes (Jia et al. 2008).

We conclude by pointing out that monitoring the time variations of the pulsed fraction and the burst rate is an important element in revealing the burst mechanism. This will be achieved by wide field detectors such as the Monitor of All-sky X-ray Image (MAXI) on-board the international space station (Matsuoka et al. 1997).

---

[5]   The reports are available on http://www.astro.isas.jaxa.jp/suzaku/process/caveats/caveats_xrtxis06.html.

[6]   The burst list is available on http://www.ssl.berkeley.edu/ipn3/sgrlist.txt.
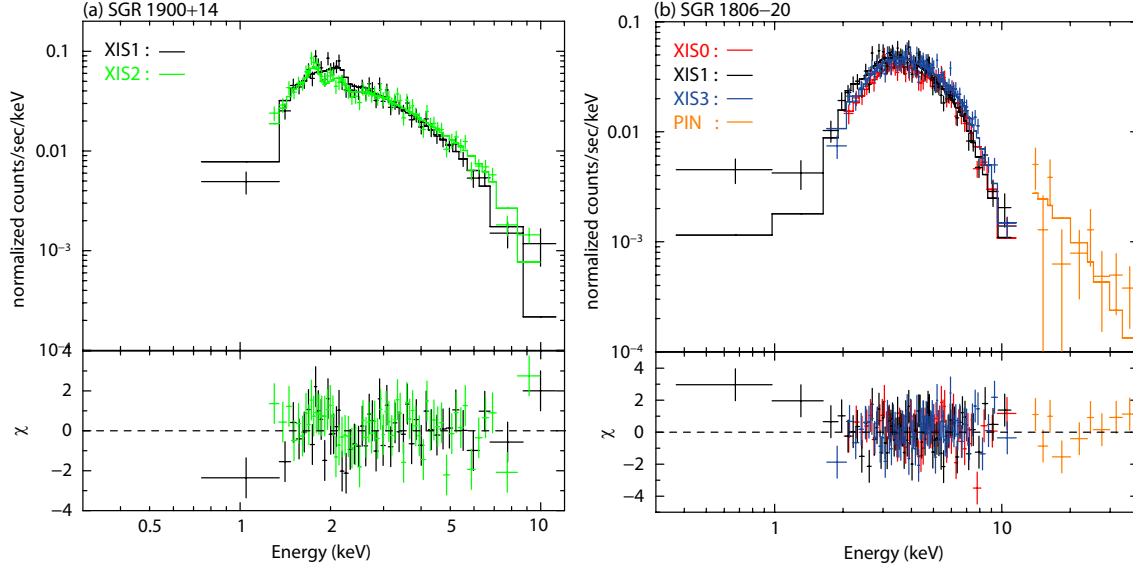
Fig. 1. Quiescent emission spectra of SGR 1900+14 (a) and SGR 1806−20 (b).
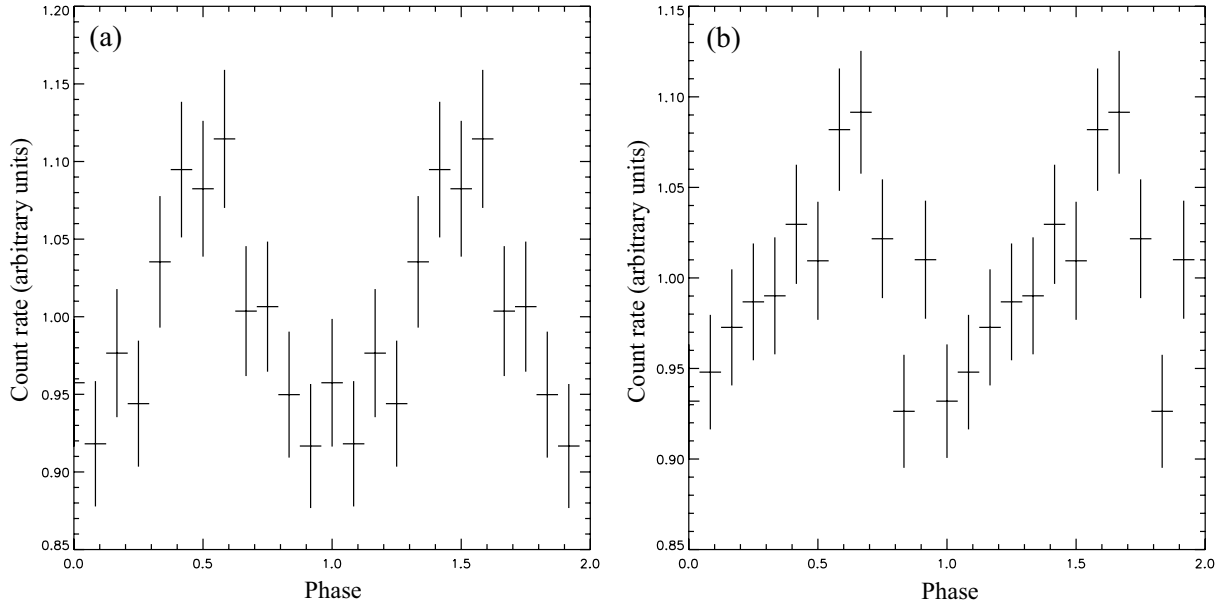

Fig. 2. Folded 0.2-12 keV light curves for SGR 1900+14 (a) and SGR 1806−20 (b).

Table 1. A summary of *Suzaku* ToO observations.

SGR	SeqNum*	Observation Date (MJD)		$T^\dagger$	XIS‡	Regions§	
		Start	End	(ks)		FI	BI
1900+14	401022010	53826.363	53826.911	17.0	1, 2	$2\rlap{.}'3 \times 5\rlap{.}'0 / 2\rlap{.}'3 \times 6\rlap{.}'7$	$2\rlap{.}'3 \times 7\rlap{.}'0 / 2\rlap{.}'3 \times 3\rlap{.}'2$
1806−20	401021010	54189.631	54190.063	19.6	0, 1, 3	$2\rlap{.}'2 \times 5\rlap{.}'3 / 2\rlap{.}'2 \times 3\rlap{.}'7$	$2\rlap{.}'2 \times 7\rlap{.}'0 / 2\rlap{.}'2 \times 3\rlap{.}'5$

* *Suzaku* sequence number.
† Net exposure time for each observation.
‡ XIS sensor number.
§ Extracted source/background regions for front-illuminated (FI) and back-illuminated (BI) CCDs.
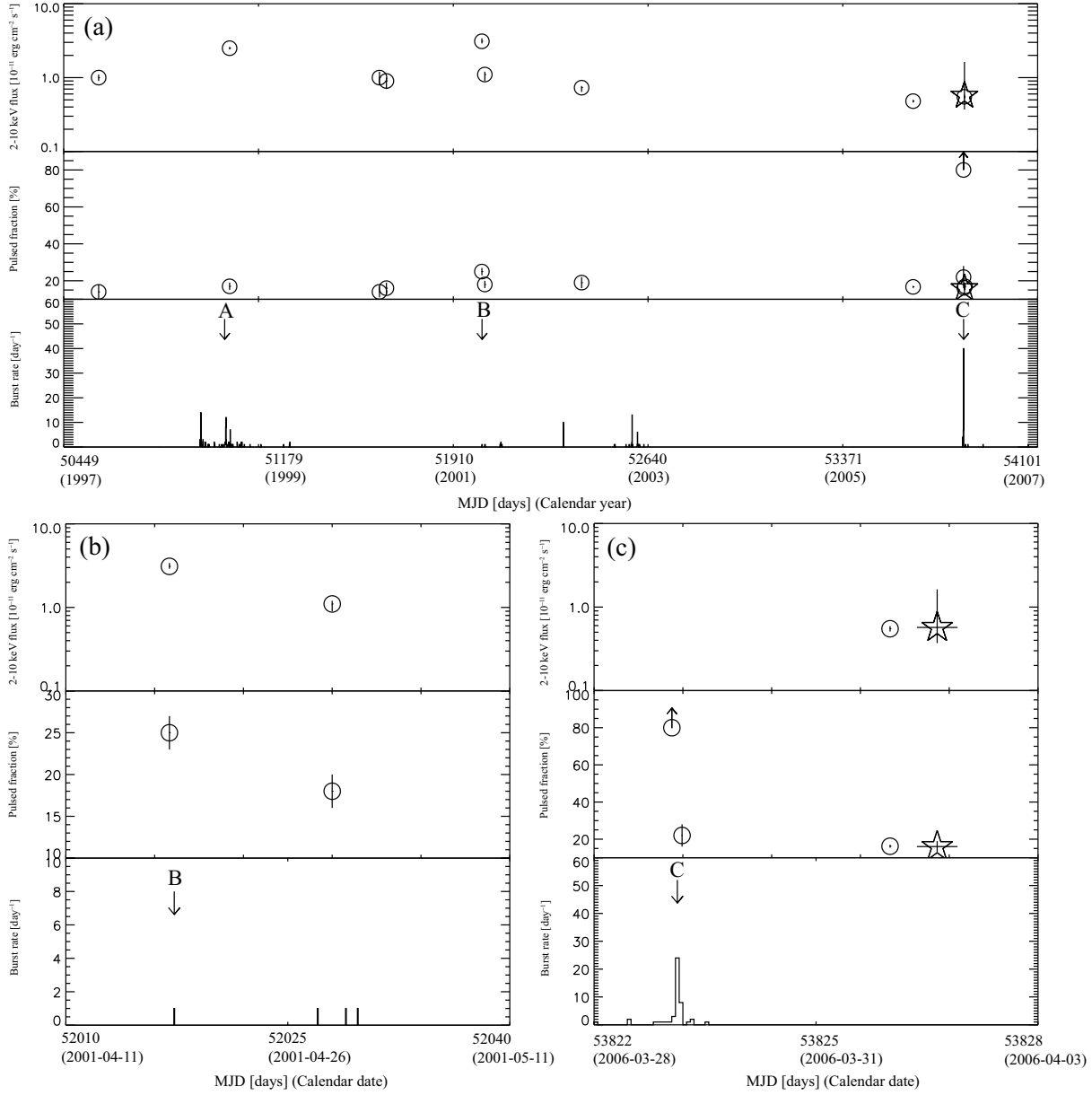
Fig. 3. Panel (a): time variations of the 2-10 keV flux, the pulsed fraction and the burst rate from 1997 to 2007, where A, B and C indicate the days of the giant flare on 27 August 1998, the intermediate flare on 18 April 2001 and the extraordinary burst activity with more than 40 bursts on 29 March 2006, respectively. Panels (b) and (c): expanded plots around the days of B and C, respectively. The *Suzaku* observation is plotted with star symbols.

Table 2. A summary of timing analyses.

SGR	Epoch (MJD TDB)	P^*	$\dot{P}^\dagger$
1900+14	53826.001	5.1998 ± 0.0002	8.7 ± 1.2
1806−20	54189.0009	7.6022 ± 0.0007	75 ± 4

* Pulse periods in units of s.
† Pulse period derivatives in units of $10^{-11}\,\mathrm{s\,s^{-1}}$.

Table 3. A summary of spectral parameters. The XIS spectra of SGR 1900+14 are fitted with 2BB or BB+PL, while the XIS and PIN diodes spectra of SGR 1806−20 are fitted with 2BB+HPL or BB+PL+HPL. The spectral parameters of the non-thermal hard emission of SGR 1806−20 are not shown in the table because the index and the flux were fixed to $\Gamma = 1.6$ and $F = 2.9 \times 10^{-11}\,\mathrm{erg\,cm^{-2}\,s^{-1}}$ (see subsection 3.2), respectively.

SGR	Model	$N_{\mathrm{H}}{}^{*}$ $(10^{22}\,\mathrm{cm}^{-2})$	$kT_{\mathrm{LT}}\ (kT_{\mathrm{BB}})^{\dagger}$ (keV)	$R_{\mathrm{LT}}\ (R_{\mathrm{BB}})^{\ddagger}$ (km)	$kT_{\mathrm{HT}}{}^{\dagger}$ (keV)	$R_{\mathrm{HT}}{}^{\ddagger}$ (km)	$\Gamma^{\S}$	$F^{\|}$	χ^2 (d.o.f.)
1900+14	2BB	2.2 ± 0.3	0.49 ± 0.06	$4.6^{+1.7}_{-1.0}$	$1.5^{+0.3}_{-0.2}$	$0.36^{+0.16}_{-0.11}$	$\cdots$	4.1 ± 0.5	115 (105)
	BB+PL	$3.2^{+0.9}_{-0.7}$	$0.29^{+0.17}_{-0.10}$	$12.3^{+71.8}_{-9.3}$	$\cdots$	$\cdots$	$2.8^{+0.3}_{-0.5}$	4.1 ± 0.5	106 (105)
1806−20	2BB+HPL	$7.8^{+1.2}_{-0.9}$	$0.54^{+0.08}_{-0.09}$	$3.1^{+2.7}_{-1.3}$	$2.7^{+3.4}_{-1.1}$	$0.06^{+0.19}_{-0.04}$	$\cdots$	9.9 ± 1.6	196 (192)
	BB+PL+HPL	$8.0^{+2.0}_{-1.1}$	$0.51^{+0.09}_{-0.13}$	$3.6^{+5.9}_{-1.6}$	$\cdots$	$\cdots$	$1.6^{+2.2}_{-1.1}$	9.9 ± 1.6	196 (192)

* N_{H} denotes the photoelectric absorption with 90% confidence level errors.

† kT_{LT}, kT_{HT} and kT_{BB} denote blackbody temperatures with 90% confidence level errors.

‡ R_{LT}, R_{HT} and R_{BB} denote the emission radius with 90% confidence level errors.

§ Γ denotes the power law index with 90% confidence level errors.

$^{\|}$ F denotes the 2-10 keV flux in units of $10^{-12}\,\mathrm{erg\,cm^{-2}\,s^{-1}}$ with 68% confidence level errors.

References

Atteia, J. -L. et al. 2003, in Gamma-Ray Bursts and Afterglow Astronomy, ed. G. R. Ricker & R. Vanderspek (Melville: AIP), 662, 17

Bamba, A. et al. 2007, PASJ, 59, S209

Bibby, J. L. et al. 2008, MNRAS, 386, L23

Boldt, E. 1987, IAU Circ., 124, 611B

Cameron, P. B. et al. 2005, Nature, 434, 1112

Cea, P. 2006, A&A, 450, 199

Corbel, S., Wallyn, P., Dame, T. M., Durouchoux, P., Mahoney, W. A., Vilhu, O., & Grindlay, J. E. 1997, ApJ, 478, 624

Corbel, S., & Eikenberry, S. S. 2004, A&A, 419, 191

Duncan, R., & Thompson, C. 1992, ApJ, 392, L9

Esposito, P. et al. 2007, A&A, 476, 321

Feroci, M. et al. 2003, ApJ, 596, 470

Frail, D. A., Kulkarni, S. R., & Bloom, J. S. 1999, Nature, 398, 127

Golenetskii, S. et al. 2007, GRB Coord. Netw. Circ., 6228

Güver, T., Özel, F., & Lyutikov, M. 2006, arXiv: astro-ph/0611405

Hurley, K., et al. 1999, ApJ, 510, L111

Hurley, K., et al. 2005, Nature, 434, 1098

Ibrahim, A. I., Safi-Harb, S., Swank, J. H., Parke, W. P., Zane, S., & Turolla, R. 2002, ApJL, 574, L51

Israel, G. L. et al. 2008, arXiv: astro-ph/0805.3919

Jia, J. J., Huang, Y. F., & Cheng, K. S. 2008, ApJ, 677, 488

Kouveliotou, C. et al. 1999, ApJL, 510, L115

Koyama, K., et al. 2007, PASJ, 59, S23

Matsuoka, M., et al. 1997, SPIE, 3114, 414

McClure-Griffiths, N. M., & Gaensler, B. M. 2005, ApJ, 630, L161

Mereghetti, S., et al. 200, ApJ, 653, 1423

Mitsuda, K., et al. 2007, PASJ, 59, S1

Molkov, S., Hurley, K., Sunyaev, R., Shtykovsky, P., Revnivtsev, M., & Kouveliotou, C. 2005, A&A, 433, L13

Nakagawa, Y. E. et al. 2007a, PASJ, 59, 653

Nakagawa, Y. E., Yoshida, A., Yamaoka, K., & Shibazaki, N. 2007b, arXiv: astro-ph/0710.3816

Nakagawa, Y. E., Sakamoto, T., Sato, G., Gehrels, N., Hurley, K., & Palmer, D. M. 2008, ApJL, 681, L89

Ricker, G., et al. 2003, in Gamma-Ray Bursts and Afterglow Astronomy, ed. G. R. Ricker & R. Vanderspek (Melville: AIP), 662, 3

Paczyński, B. 1992, Acta Astron., 42, 145

Perna, R., Heyl, J. S., Hernquist, L. E., Juett, A. M., & Chakrabarty, D. 2001, ApJ, 557, 18

Rea, N., Israel, G. L., Stella, L., Oosterbroek, T., Mereghetti, S., Angelini, L., Camapana, S., & Covino, S. 2003, ApJL, 586, L65

Serlemitsos, P. J. et al. 2007, PASJ, 59, S9

Takahashi, T., et al. 2007, PASJ, 59, S35

Thompson, C., & Duncan, R. 1995, MNRAS, 275, 255

Terasawa, T., et al. 2005, Nature, 434, 1110

Vrba, F. J., Henden, A. A., Luginbuhl, C. B., Guetter, H. H., Hartmann, D. H., & Klose, S. 2000, ApJ, 533 L17

Winkler, C. 1999, Astrophysics Letters & Communications, 39, 309

Woods, P. M., & Thompson, C. 2006, in Compact Stellar X-ray Sources, ed. W. Lewin & M. van der Klis (Cambridge: Cambridge Univ. Press), 547

Woods, P. M., Kouveliotou, C., Finger, M. H., Göğüş, E., Wilson, C. A., Patel, S. K., Hurley, K., & Swank, J. H. 2007, ApJ, 654, 470